Long-tailed distribution of excitatory postsynaptic potentials enhances learning performance of Liquid State Machine

Ibuki Matsumoto†, Sou Nobukawa†‡, Nobuhiko Wagatsuma⋆, and Tomoki Kurikawa∗

† Chiba Institute of Technology, 2-17-1 Tsudanuma, Narashino, Chiba 275–0016, Japan
‡ National Center of Neurology and Psychiatry, 4-1-1 Ogawahigasicho, Kodaira, Tokyo 187–8551, Japan
⋆ Toho University, 2-2-1 Miyama, Funabashi, Chiba 274–8510, Japan.
∗ Kansai Medical University, 2-5-1 Hirakata, Shinmachi, Osaka 573–1010, Japan
Email: s1931144ZL@s.chibakoudai.jp (IM), nobukawa@cs.it-chiba.ac.jp (SN)

Abstract—In the cerebral cortex, excitatory postsynaptic potentials (EPSPs) exhibit a long-tailed distribution. EPSPs increase the membrane potentials of postsynaptic neurons, and it is known that the long-tailed characteristic of EPSPs induces spontaneous activity and stochastic resonance in the cerebral cortex. Spiking neural networks with the long-tailed characteristics of EPSPs result in spontaneous deterministic dynamics. In this context, we hypothesized that a long-tailed distribution of EPSPs would improve the learning performance of machine learning. Therefore, we constructed the liquid state machine (LSM), which is one type of a reservoir computing model. We leveraged a spiking neural network with long-tailed characteristics of EPSPs as a reservoir in LSM, and then evaluated the learning performance of LSM via a memory capacity task. We found that long-tailed distributions of EPSPs enhance the high memory capacity. This finding might help improve the learning performance of LSM.

1. Introduction

Neural networks in the brain, which consist of large-scale neural populations, realize advanced cognitive functions, such as learning, memory, and perception [1]. Such cognitive functions are performed by dynamic interactions among many brain areas [2]. These dynamics involve spatio-temporal fluctuations across several hierarchical scale levels, which can enhance brain functions; this is known as stochastic resonance [1]. The mechanism for this enhancement has been investigated using physiological, experimental, and computational approaches [3]. In addition to the multi-scale neural fluctuations, the mechanism to produce microcircuit level fluctuation in the cerebral cortex has also been studied [4].

Fluctuations at the microcircuit level are generated by the interactions among neurons [4]. In the cerebral cortex, neurons fire irregularly even in the absence of a stimulus; the firing rates are no more than 1 Hz, which represents very low-frequency activity in the brain [4]. This

neural activity is called "spontaneous activity". A model-based study by Teramae et al. demonstrated that this spontaneous activity is generated by long-tailed distributions of excitatory postsynaptic potentials (EPSPs) in the cerebral cortex [4]. Experimental studies evaluated the connections between excitatory neurons in the cortex and found many weak synaptic connections and a few large-amplitude synaptic connections [5, 6]. The mapping of EPSPs amplitudes suggests that their distributions follow a lognormal distribution. In the long-tailed distribution of EPSPs, many weak synaptic connections help transmit spikes received from a few strong synapses faithfully; that is, a few strong synaptic connections play the role of a signal, whereas the many weak ones as a background noise to raise the baseline activity. In this way, the coexistence of many weak synaptic connections and a few strong synaptic connections creates stochastic resonance and greatly contributes to information processing in the microcircuits of the cortex. In the study focusing on the characteristics of long-tailed EPSPs, the mechanism of stochastic resonance promoted memory recall in an associative memory (AM) model [7]. In the AM model, internal noise works effectively to retrieve the embedded memory pattern [7]. In other words, spontaneous activity with slow temporal-scale behaviors makes memory-retrieving neurons prone to depolarization. Thus, in the case where the neuron-embedded memory patterns receive input through a strong synapse, neurons can evoke spikes or retrieve memory. In addition, our recent studies have shown that these neural activities produced by the long-tailed distribution of EPSPs involve deterministic properties in spatio-temporal spiking patterns [8, 9]. The use of these complex spike patterns in machine learning has been previously proposed [10].

Reservoir computing is a computational framework that enables high-speed machine learning derived from recurrent neural network models. Echo state networks (ESN) and liquid state machines (LSM) are typical reservoir computing models [11, 12]. These models have a three-layer structure, consisting of input, reservoir, and output layers, and the node weights are updated only in the output layer. Therefore, high-speed learning is possible. LSM is a mathematical model that emerged from computational neuro-

ORCID iDs Ibuki Matsumoto: 0000-0002-3501-5304, Sou Nobukawa: 0000-0001-7003-6912, Nobuhiko Wagatsuma: 0000-0001-9090-9223, Tomoki Kurikawa: 0000-0003-1475-2812

science, and it aims to elucidate the computational properties of neural circuits. Therefore, a spiking neural network with biological properties is used in the reservoir layer. As discussed, the long-tailed distribution of EPSPs is widely observed in the neural system; hence, we can apply it to LSM and evaluate its effect on learning performance.

In this context, we hypothesized that the long-tailed distribution of EPSPs, which plays an important role in supporting brain function, would contribute to the performance of LSM. To prove this hypothesis, we constructed an LSM using a spiking neural network that considers the distributional characteristics of EPSPs that generate spontaneous activity. The difference between the two models, with and without the long-tailed distributions of EPSPs, was compared and evaluated in a memory capacity task.

2. Method

2.1. Liquid State Machine

In this study, we built an LSM consisting of a spiking neural network with a long-tailed distribution of EPSPs. An overview of the LSM is shown in Fig.1. The dynamics of each neuron follow a leaky integrate-and-fire model. The LSM consists of an input, reservoir, and output layers. The input layer consists of N_{in} =20 excitatory neurons, and the reservoir layer consists of N_E =10000 excitatory neurons and N_I =2000 inhibitory neurons. The excitatory neurons in the reservoir layer were classified into 100 neural populations. The output layer consists of synaptic weight W_{out} from the neural populations in the reservoir layer to the output of LSM.
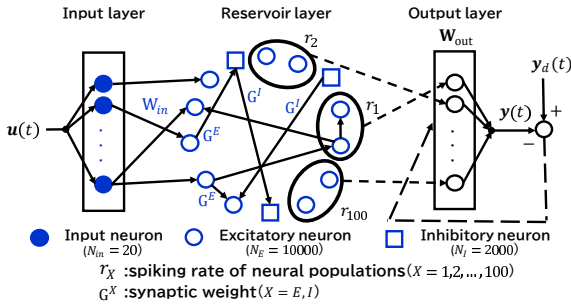

Figure 1: Liquid state machine with the long-tailed distribution of EPSPs. A spiking neural network with a random topology is used in the reservoir layer.

The input neurons receive external input $u(t)$ and provide spikes to the reservoir neurons. The membrane potential $v_i(t)(i = 1, 2, ..., 20)$ of the input neuron that receives an external input is as follows:

$$\frac{dv_i}{dt} = -\frac{1}{\tau_{in}}(v_i - V_L) + u(t), \tag{1}$$

$$\text{if } v \geq V_{thr} \text{ mV, then } v(t) \to V_r. \tag{2}$$

Here, τ_{in} is the decay constant of the membrane ($\tau_{in} = 20$ [ms]), V_L is the leak current ($V_L = -70$ [mV]), and $u(t)$ is the external input generated by uniform random numbers [0, 0.01]. This random value of the external input $u(t)$ changes every 1 [ms]. Input neurons fire when the membrane potential exceeds the threshold value of V_{thr} (= -50 [mV]). After spiking, the membrane potentials were reset to the reset potential V_r (= -60 [mV]). The dynamics of the membrane potential $v_j(t)$ of the excitatory neurons ($j = 1, 2, ..., N_E$) and inhibitory neurons ($j = N_E + 1, ..., N_E + N_I$) in the reservoir layer are as follows:

$$\frac{dv_j}{dt} = -\frac{1}{\tau_m}(v_j - V_L) - g_{E,j}(v_j - V_E) - g_{I,j}(v_j - V_I)$$
$$+ \sum_i W_{j,i}^{in} \sum_{S_i} \delta(t - s_i). \tag{3}$$

Here, the decay constant of the membrane τ_m is 20 [ms] for excitatory neurons and 10 [ms] for inhibitory neurons, and the excitatory synaptic current, inhibitory synaptic current, and leak current are $V_E = 0$ [mV], $V_I = -80$ [ms], $V_L = -70$ [mV], respectively. In addition, the input neurons and reservoir neurons were randomly connected with coupling probabilities of 0.1. $\delta(t)$ is a delta function. That is, when reservoir neurons receive spikes from i-th input neurons at time $t = s_i$, the membrane potentials of the reservoir neurons increase W_{in} [mV], and we set $W_{in} = 1.0$ [mV]. Reservoir neurons also have a threshold potential V_{thr} and reset potential V_r, according to Eq.(2). The conductance for the excitatory synapse $g_{E,j}(t)[\text{ms}^{-1}]$ and inhibitory synapse $g_{I,j}(t)[\text{ms}^{-1}]$ is as follows:

$$\frac{dg_{X,j}}{dt} = -\frac{g_{X,j}}{\tau_s} + \sum_k G_k^X \sum_{S_k} \delta(t - s_k - d_k), \; X = E, I. \tag{4}$$

Here, τ_s is the decay constant of the membrane ($\tau_s = 2$ [ms]). s_k is the spike time of the input from k-th neuron, and d_k is the synaptic delay. In addition, G_k^E and G_k^I are the excitatory synaptic weight and the inhibitory synaptic weight, respectively. That is, when the k-th presynaptic neuron fires at time $t = (s_k + d_k)$, the spike weighted by G_k^X is transmitted to the j-th postsynaptic neuron. As previously stated, EPSP shows a long-tailed distribution defined as:

$$p(x) = \frac{\exp[-(\log x - \mu)^2/2\sigma^2]}{\sqrt{2\pi}\sigma x}, \tag{5}$$

where, x is the amplitude of EPSPs. In this case, we set the values $\sigma = 1.0$ and $\mu = 1 + \log(0.2)$. We defined EPSP ≤ 2 [mV] as the weak synaptic weight and EPSP > 2 [mV] as the strong synaptic weight. This strong weight is called as the long-tailed part of EPSP. In addition, we reduced the unrealistic value of EPSPs (≥ 20 [mV]) and recalculated a new value. Because the EPSP is an observable value, it must be translated into a synaptic weight G_k^E. We translated EPSP into G_k^E based on our previous

study, which treated the relationship between EPSP and G_k^E : G_k^E = $V_{\text{EPSP}}/100$ [8]. The value of the synaptic weight was set to G_j^E = 0.018 (excitatory-to-inhibitory), to G_j^I = 0.002 (inhibitory-to-excitatory), and to G_j^I = 0.0025 (inhibitory-to-inhibitory). In addition, the connection probabilities we set were 0.1 (excitatory-to-inhibitory) and 0.5 (others, except for the connection between excitatory-to-excitatory). Also, the values of synaptic delays were set randomly between 1-3 [ms] (excitatory-to-excitatory) and 0-2 [ms] (other connections).

In this study, we numerically simulated neural activity for 50 [s]. To quantify neural activity, we calculated the number of spikes per 0.1 [ms] in the excitatory neural population. That is, we obtained the average spiking rate r_X (X = 1, 2, 3, ..., 100) [Hz] of the neural population consisting of excitatory neurons that were classified into 100 groups by simulation.

$$r_X(t) = 10^3 \frac{S_X(t)}{100\Delta t}, \; X = 1, 2, 3, ..., 100. \tag{6}$$

Here, S_X is the spike frequency with a bin size of 0.1 [ms] in the X-th neural population (spikes/0.1 [ms]). We smoothed the rate values r_X [Hz] using a Gaussian filter with a window size of 10 [ms]. To obtain an optimized output corresponding to the input, the LSM must be trained. W_{out} was updated using the ridge regression algorithm as follows:

$$W_{\text{out}} = ((X^\mathsf{T} X + \alpha I)^{-1} X^\mathsf{T} D)^\mathsf{T}. \tag{7}$$

Here, α and I indicate the non-negative regularization coefficient, the identity matrix, respectively. X = $(r_X(1), ..., r_X(T))^\mathsf{T}$ is the spiking rate of the 100 neural populations that state the collection matrix ($T \times 100$). T indicate the learning duration. Furthermore, D = $(y_d(1), ..., y_d(T))^\mathsf{T}$ denote the desired output collection matrix ($T \times 1$). Finally, the output $y(t)$ of LSM is given as

$$y(t) = W_{\text{out}} \times X. \tag{8}$$

In this study, α = 0.01 because the memory capacity is maximized in both cases with and without strong weights. One trial of simulation duration consisted of the first transient period of 500 [ms], the learning duration of T = 49000 [ms], and the last transient period of 500 [ms].

2.2. Evaluation Index

We evaluated the learning performance of LSM in a memory capacity task [13]. In the memory capacity task, an input series $u(t)$ is a uniform distribution over [0, 0.01], and the desired series is the input one τ-time step before. In other words, the desired signal $y_d(t) = u(t - \tau)$ was used to train the input $u(t)$. $y(t)$ is the output series of LSM following Eq.(8). The memory capacity (MC_τ) is given by

$$\text{MC}_\tau = \frac{\text{cov}^2(\mathbf{u}_\tau, \mathbf{y})}{\sigma^2(\mathbf{u}_\tau)\sigma^2(\mathbf{y})}. \tag{9}$$

Here, $\text{cov}(\mathbf{u}_\tau, \mathbf{y})$ indicates the covariance between $\mathbf{u}_\tau$ and $\mathbf{y}$. σ^2 indicates the variance. We set 1 [ms] $\leq \tau \leq$ 1000 [ms]. MC_τ exhibits a value between 0 and 1. When MC_τ approaches 1, LSM retains a large amount of information from the previous τ step.

3. Result

Figure2 shows the forgetting curve of the τ-delay memory capacity in cases with and without strong weights. The LSM with a strong weight exhibited a high memory capacity ($\text{MC}_\tau \approx 0.97$) in $0 \leq \tau \leq 10$ [ms], whereas the LSM without a strong weight exhibited a low memory capacity ($\text{MC}_\tau \approx 0.48$). This means that the characteristics of long-tailed EPSPs contribute to retaining previously learned information.
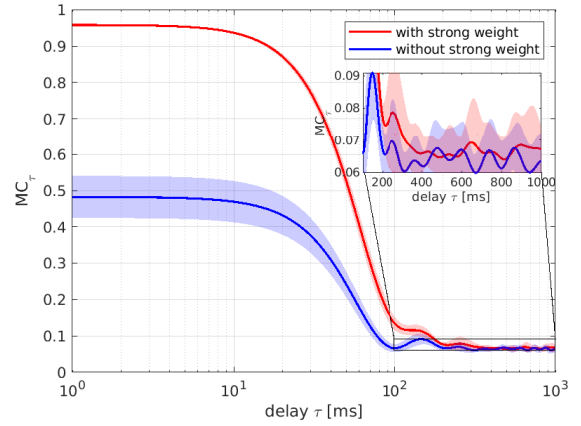

Figure 2: Forgetting curve on delay τ [ms] of memory capacity task in the case with strong weights (indicated by the red line) and without strong weights (indicated by the blue line). The line and the shadow indicate an "average of forgetting" curve and standard deviation over 10 trials of the memory capacity task. Here, external input spikes according to the Poisson process with a spiking rate of 5 [Hz] are given to the all-reservoir neurons in the case without strong weights. By this effect, the spiking rate of neural populations become same in comparison with strong synaptic weights.

4. Discussion

In this study, we hypothesized that the long-tailed characteristics of EPSPs can improve learning performance based on previous studies on LSM [4, 7, 8]. To verify this hypothesis, we constructed an LSM by using a leaky integrate-and-fire spiking neural network with a long-tailed distribution of EPSPs. The LSM that has both strong and weak weights at the connection of excitatory-to-excitatory neurons, can achieve a higher memory capacity than one without strong weights. We must consider why strong

synaptic connections achieve high memory capacity. We know that strong synaptic connections can transmit information to various pathways, such as long and short paths, whereas weak synaptic connections can only transmit information to short paths. Therefore, if the spiking neural network involves strong synaptic connections, a recurrent network is generated; that is, dynamic behavior with a long decay factor is produced. These dynamics contribute to enhancing memory capacity (see Fig.2). This finding suggests that strong spatial synapses play an important role in information processing.

Regarding the future directions of this research, we need to evaluate the nonlinear time-series prediction for the LSM that we constructed to increase memory capacity by the long-tailed distribution of EPSPs in machine learning. In addition, in this study, we used spiking rate coding for LSM, but the widely utilized spike coding in LSM is timing coding [14, 15]. Hence, we must use timing coding for the learning of LSM in future studies.

In conclusion, we found that the long-tailed distribution of EPSPs contributes to high memory capacity. This finding may be widely used to enhance the abilities of LSM.

Acknowledgments

References

[1] Olaf Sporns. *Networks of the Brain*. MIT press, 2016.

[2] Steven L Bressler and Vinod Menon. Large-scale brain networks in cognition: emerging methods and principles. *Trends in cognitive sciences*, Vol. 14, No. 6, pp. 277–290, 2010.

[3] Frank Moss, Lawrence M Ward, and Walter G Sannita. Stochastic resonance and sensory information processing: a tutorial and review of application. *Clinical neurophysiology*, Vol. 115, No. 2, pp. 267–281, 2004.

[4] Jun-nosuke Teramae, Yasuhiro Tsubo, and Tomoki Fukai. Optimal spike-based communication in excitable networks with strong-sparse and weak-dense links. *Scientific reports*, Vol. 2, No. 1, pp. 1–6, 2012.

[5] Sandrine Lefort, Christian Tomm, J-C Floyd Sarria, and Carl CH Petersen. The excitatory neuronal network of the c2 barrel column in mouse primary somatosensory cortex. *Neuron*, Vol. 61, No. 2, pp. 301–316, 2009.

[6] Andreas Frick, Dirk Feldmeyer, Moritz Helmstaedter, and Bert Sakmann. Monosynaptic connections between pairs of l5a pyramidal neurons in columns of juvenile rat somatosensory cortex. *Cerebral cortex*, Vol. 18, No. 2, pp. 397–406, 2008.

[7] Naoki Hiratani, Jun-Nosuke Teramae, and Tomoki Fukai. Associative memory model with long-tail-distributed hebbian synaptic connections. *Frontiers in computational neuroscience*, Vol. 6, p. 102, 2013.

[8] Sou Nobukawa, Nobuhiko Wagatsuma, and Haruhiko Nishimura. Deterministic characteristics of spontaneous activity detected by multi-fractal analysis in a spiking neural network with long-tailed distributions of synaptic weights. *Cognitive Neurodynamics*, Vol. 14, No. 6, pp. 829–836, 2020.

[9] Sou Nobukawa, Haruhiko Nishimura, Nobuhiko Wagatsuma, Satoshi Ando, and Teruya Yamanishi. Long-tailed characteristic of spiking pattern alternation induced by log-normal excitatory synaptic distribution. *IEEE Transactions on Neural Networks and Learning Systems*, Vol. 32, No. 8, pp. 3525–3537, 2020.

[10] Guillaume Bellec, Darjan Salaj, Anand Subramoney, Robert Legenstein, and Wolfgang Maass. Long short-term memory and learning-to-learn in networks of spiking neurons. *Advances in neural information processing systems*, Vol. 31, pp. 787–797, 2018.

[11] Herbert Jaeger. The "echo state" approach to analysing and training recurrent neural networks-with an erratum note. *Bonn, Germany: German National Research Center for Information Technology GMD Technical Report*, Vol. 148, No. 34, p. 13, 2001.

[12] Wolfgang Maass, Thomas Natschläger, and Henry Markram. Real-time computing without stable states: A new framework for neural computation based on perturbations. *Neural computation*, Vol. 14, No. 11, pp. 2531–2560, 2002.

[13] Herbert Jaeger. *Tutorial on training recurrent neural networks, covering BPPT, RTRL, EKF and the" echo state network" approach*, Vol. 5. GMD-Forschungszentrum Informationstechnik Bonn, 2002.

[14] Yong Zhang, Peng Li, Yingyezhe Jin, and Yoonsuck Choe. A digital liquid state machine with biologically inspired learning and its application to speech recognition. *IEEE transactions on neural networks and learning systems*, Vol. 26, No. 11, pp. 2635–2649, 2015.

[15] Benjamin Schrauwen, MichielD'Haene, David Verstraeten, Jan Van Campenhout. Compact hardware liquid state machines on FPGA for real-time speech recognition. *Neural networks*, Vol. 21, No. 2-3, pp. 511–523, 2008.